2014 IEEE International Conference on Robotics & Automation (ICRA)
Hong Kong Convention and Exhibition Center
May 31 - June 7, 2014. Hong Kong, China

Design and Implementation of an Illumination System for Microrobotic Paper Fiber Studies

Juha Hirvonen, Antti Hänninen, and Pasi Kallio, *Member, IEEE*

***Abstract*— This paper discusses design and implementation of an illumination system for microrobotic manipulation of natural fibrous materials, such as paper fibers. Three different illumination types potentially suitable for this imaging task are discussed and prototypes are built for further testing. The final illumination system is implemented based on the test results. It uses polarized light and it is integrated to the sample holder of a microrobotic platform. The final system provides an excellent contrast between the fibers and the background.**

I. Introduction

Paper fibers are the main component of paper and thus, the mechanical properties of paper are mainly described by the mechanical properties of the paper fibers and paper fiber bonds. Therefore, understanding the properties of the paper fibers and their bonding capabilities will contribute in improving paper quality. Conventionally, test sheets and sample portions of pulp are used for estimating the bond strength and mechanical composition of fibers. However, due to the complex structure of the samples, the obtained average parameters include also undesired components. To provide reliable fiber level data, the paper fiber properties should be measured from individual fibers. With traditional methods and devices, this is slow and laborious work with a low yield.

The Micro- and Nanosystems Research Group at Tampere University of Technology has developed a microrobotic platform for manipulation and measurement of individual paper fibers. The platform has been used in flexibility measurements of individual paper fibers [1] and bonding strength measurements of individual paper fiber bonds [2]. The platform consists of i) a sample holder including a rotary table for angular movement and an xy table for Cartesian movement, ii) 3-DOF microgrippers for grasping the fibers and iii) a microforce sensor for flexibility or bonding strength measurements. All the actuators are manufactured by SmarAct, Germany, and the force sensor is manufactured by Femto Tools Inc., Switzerland. A camera is attached on top of the platform to provide visual feedback to the user. The camera and the optics are manufactured by AVT, USA, and Navitar, USA, respectively. There is a coaxial bright light illuminator integrated to the optics. The devices in the platform are operated by a tailor-made user interface. Fig. 1 presents the platform and a sample view from the camera.

The research goal is to automate the measurement protocols of the platform to achieve a high yield. Machine vision will be used as the feedback system giving information of the fiber and gripper positions. In all the measurements, the first step is to detect the fibers placed on the sample holder and choose the most suitable ones for the tests. For this, all the fibers should be clearly seen in the images captured. The coaxial bright light illuminator produces uneven lighting, which does not meet this condition.

Proper illumination is extremely important for micromanipulation tasks under an optical microscope. Illumination has to be adjusted based on the properties and the shape of the parts to be manipulated and the platform to be used. [3]. Fibers are challenging for illumination for four reasons. Firstly, the fibers are small in size (couple of millimeters in length and couple of tens of micrometers in diameter) and transparent to some extent. Secondly, the fibers can be either dry or immersed in a thin layer of water, and the liquid may cause reflections. Thirdly, the image area should be relatively large for sufficiently high number of fibers to fit in it. In previous tests [1, 2], a circular area with a diameter of 19 mm has been used. Fourthly, the actuators – especially the grippers – constrain placing the light sources and may cast shadows. Also, the illumination system should allow the sample holder to rotate and move in x and y directions.

Both academia and industry have done plenty of research work for evaluation of paper fiber properties by photography

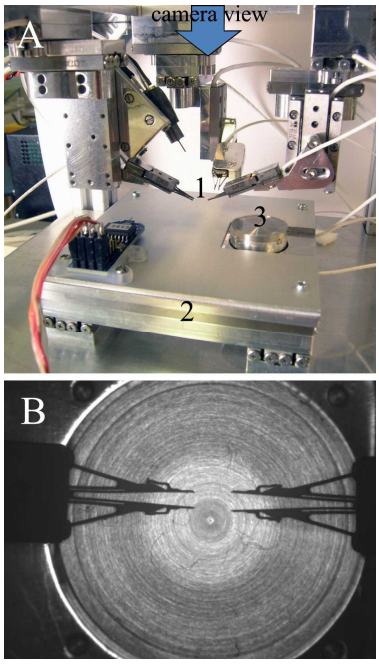

Figure 1. The platform (A): 1 – microgrippers, 2 – xy table, 3 – rotary table, camera view (B).

Juha Hirvonen, Antti Hänninen, and Pasi Kallio are with Department of Automation Science and Engineering, Tampere University of Technology, Tampere, FIN-33720 Finland (phone: +358 50 300 8154; e-mail: juha.hirvonen@tut.fi).

and computer vision [4-9]. However, the illumination schemes presented in the current literature are not applicable to our problem.

Hirn [4] presents six widely used commercial fiber analyzers in his review. All of them are based on pumping the fibers in suspension through a transparent narrow flow cell, in which they are photographed with one or multiple high speed cameras. The image area can be as small as 0.5mm * 0.5mm, and high-power rear illumination is used in all of the analyzers. The measured parameters include fiber length, width, curl and coarseness. Tiikkaja [5] uses one of the analyzers and a flow fractionator to study the effect of morphological properties of fibers on the quality of thermomechanical pulp.

Echart [6] presents a method to estimate fiber flexibility in a flow cell with a cross junction, where the flow deforms the fiber. High power LED is used for illumination. The image processing steps include background subtraction, binarization and skeletonization to calculate fiber parameters.

Reme [7] evaluated the changes in the fibers in the refining process from wood to finished paper by using scanning electron microscopy (SEM). The work included image analysis algorithms for estimating fiber length, cross-section and surface quality.

Coeurjolly [8] and Axelsson [9] report tracking and curvature estimation of fibers in 3D images of paper. They use either a sectioning device and SEM, or X-ray microtomography in image acquisition. Image processing includes e.g. centerline approximation.

Hence, all of the presented studies involve computer vision algorithms for paper fiber analysis but the systems have been closed environments used only for gathering image data and not always based on light microscopy. The substrate has served solely as a passive background for imaging, and no external actuators have been used to manipulate the fibers. Thus, the imaging conditions differ remarkably from the ones usable in microrobotic approaches and the presented illumination solutions are not relevant for this work.

This paper presents design and implementation of an illumination system tailored for microrobotic fiber studies. The aim is to test applicability of promising existing methods, and integrate the best to the microrobotic platform. Different illumination types and building of test setups are discussed in Section II. Also, a method for evaluating the illumination is presented. The experiments and their results are presented in Section III, and the final design and implementation of the illumination system are described in Section IV. Conclusion is drawn in the end.

II. Materials and Methods

A. Illumination Test Setups

Different illumination types and the configurations of the illumination prototypes used in the experiments to find the optimal solution are presented here. The illumination types were chosen based on the similarity of their applications found in the literature to our problem. The parameters of each configuration e.g. the distance and the angle of the light source(s) were tuned by visual assessments of the images produced. In this step, the spatial constraints of the platform were not considered, as the purpose was to compare only the methods. The actual implementation and integration with the platform was considered only for the most promising method and is discussed in Section IV.

In all the tests, the fibers were placed on a transparent hydrophilic laboratory glass slide. Transparency minimizes the influence of the background. Hydrophilicity is important when wet fibers are studied since water stays as a thin layer on the slide instead of forming a dome, and thus allows the fibers stay approximately at a same level. A 100µm thick and 1mm wide polydimethylsiloxane (PDMS) ring with an inner diameter of 20mm was attached on the glass slide to create a pool for the wet samples.

1) *Dark field*

In dark field illumination, light is directed in such an angle that it is not reflected to the camera from flat surfaces. This configuration emphasizes height changes and is good for reflective surfaces. Dark field illumination has been used in detecting small details on a plane, such as surface defects [10], and applied to microscopy in analysis of yeast cells [11]. Since the fibers can be considered as narrow bumps on a surface that can be reflective (while wet), dark field illumination was a good candidate for further testing.

Two diffused SAH4 LED arrays (LATAB, Sweden) were used in prototyping the dark field illumination. The LED arrays were placed to the opposite sides of the glass slide the fibers were placed in 5cm distance. The angle of the LED arrays was approximately 90˚. Fig. 2A shows the schema of the dark field illumination test setup.

2) *Ring light*

In ring light illumination, the light sources (LEDs) are placed on a ring which surrounds the optics. The angle of the LEDs defines if the configuration utilizes bright or dark field. Thus, ring light is actually a special case of either bright or dark field illumination. Multiple light sources produce smoother illumination with less specular reflection. Therefore, it was considered a good candidate for the wet sample characterization. Ring light illumination has been previously used in the detection of small scale details from flat surfaces in applications such as printing plate surface quality analysis [12], and detection of liquid interface in microchannels [13].

The dark field ring light was the same as used in [13]. It was constructed of a metal ring with a diameter of 16.5cm and 16 bright light LEDs (Philips, Netherlands). The ring light was placed approximately 15cm above the sample fibers. The test setup schema for the ring light is seen in Fig. 2B.

3) *Polarizer – analyzer*

Polarizer – analyzer configuration uses a backlight and two polarizers: one is placed between the light source and the object and the other between the object and the camera. The second polarizer is called as an analyzer. There is an angle difference (often 90˚) between the polarizer and the analyzer. Because of the phase difference, the analyzer blocks all or majority of the light that does not pass through the object. Since the light passing through the object changes its polarity

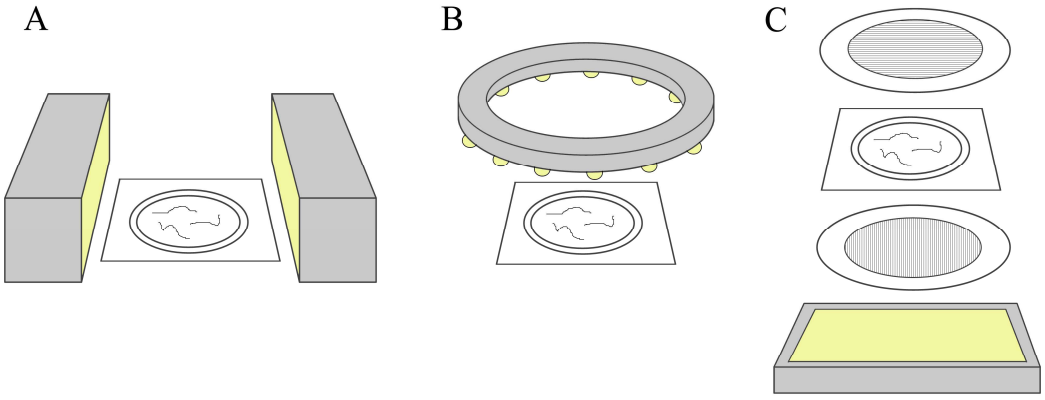

Figure 2. Schematics of the illumination test setups. Camera is located on top. Dark field (A), ring light (B) and polarizer – analyzer (C).

according to the fine structure of the object, it travels to the camera. Polarizer – analyzer is usually used in texture analysis of transparent samples and has been utilized e.g. in analysis of brain tissue [14] and cartilage [15]. Since it has been applied also to measurements of the microfibril angle [16] and the bonding area [17] of paper fibers, it is a promising candidate to this problem as well.

A 30W 5x6 LED matrix (LedHK, China) composed of surface mount LEDs was used as the light source of the polarizer – analyzer test setup. A diffuser and a polarizer (KOOD, Japan) were placed 10mm above the matrix. The glass slide for the fiber samples was placed 5mm above the polarizer. An angle difference of 90° was used to maximize the contrast between the fiber samples and the background. Fig. 2C presents the schematics of the polarizer – analyzer test setup.

B. Assessment Method

The optimal illumination should produce maximum contrast between the fiber samples and the background to facilitate segmentation. Hence, the images should have a histogram with two different sections – one representing the background and one representing the fibers. These sections should be separable with thresholding in which a binary image is produced out of a grayscale image as follows:

$$b(u,v) = \begin{cases} 1, & f(u,v) \geq T \\ 0, & f(u,v) < T \end{cases}, \quad (1)$$

where $f(u, v)$ is the original 8-bit grayscale image, $b(u, v)$ is the resulted binary image, T is the threshold, and u and v are the horizontal and vertical image coordinates. Now, the image part $b(u,v) = 1$ should consist only of the fibers and the part $b(u,v) = 0$ should describe the background.

Two thresholding methods were used in assessing the images: Otsu's automatic thresholding algorithm and a fixed threshold. Simple methods were used to weight the performance of the illumination over the performance of the thresholding algorithm. In Otsu's method, the threshold value is searched exhaustively by minimizing the intra-class variance of the suggested foreground and background pixels [18]. This method gives acceptable results when the numbers of pixels in both classes do not differ much from each other [19], and can be here used to assess how clearly separated the two histogram sections are. However, since usually the fibers cover a remarkably lower number of pixels than the background, also a fixed threshold was used as the second assessment method. The threshold value is selected based on one image. It is set as low as possible to patch the differences between and inside fiber sections in the images still avoiding causing remarkable noise in the background. The same threshold value is used for the whole image set taken with the same illumination test setup. Since the imaging conditions are kept unchanged, the same fixed threshold value is applicable to all the images.

To produce quantitative measures from the thresholded images, two ratios are calculated. Detection ratio r_{det} describes the portion of fibers preserved in the binary image. It is defined as

$$r_{det} = n_{binaryfibers} / n_{fibers}, \quad (2)$$

where $n_{binaryfibers}$ is the number of the sections in $b(u,v) = 1$ that present fibers or fiber parts with approximately at least ¾ of the pixels preserved, and n_{fibers} is the number of fibers imaged. Breakage ratio r_{break} describes the portion of the fibers detected in the binary image that have cracks or shortenings. It is defined as

$$r_{break} = n_{broken} / n_{binaryfibers}, \quad (3)$$

where n_{broken} is the number of the sections in $b(u,v) = 1$ presenting fibers or parts of them where over at least ¾ of the pixels has preserved but clear cracks or shortening can be detected. Fig. 3 presents an example of a fiber preserved, broken and lost in thresholding.

The value of r_{det} should be at least 0.90 to make the system efficient. As breakages can cause interpreting one fiber as multiple fibers, r_{break} should be low. In this study, a limit was set to 0.10. However, the breakages can be patched with morphological operations such as closing.

III. Tests and Results

Ten images of 15 – 77 fibers in a wet state on a glass slide were taken with each illumination setup. The total number of fibers imaged per setup was around 300. Unbleached softwood kraft pulp was diluted in water, and the mixture

was loaded to a pipette. Small portions of the fiber suspension were injected on the sample holder from the pipette. Thus, the number and the orientation of the fibers on the holder were random. Zoom and focus were set so that the entire PDMS ring and the fibers inside were seen sharp in the images. Exposure time was adjusted for each illumination type. The images were taken in normal laboratory conditions.

The parts of the images presenting features inside the PDMS ring were thresholded using the Otsu's method and a fixed threshold. The images were visually inspected and the parameters n_{fibers}, $n_{binaryfibers}$ and n_{broken} were counted manually and the detection ratio and the cracking ratio for each image were calculated as discussed in Section II B. Table 1 presents the used thresholds and the results and Fig. 4 shows sample images from each illumination type and the corresponding binary images thresholded by using Otsu's method and the fixed threshold.

TABLE I. ILLUMINATION TEST RESULTS

Illumination Type	r_{det}		r_{break}		T		n_{fibers}
	Otsu	*Man.*	*Otsu*	*Man.*	*Otsu*	*Man.*	
Dark field	0.16	0.63	0.56	0.61	28 – 66	31	276
Ring light	0.74	0.85	0.41	0.40	43 – 46	38	328
Polarized	0.79	0.98	0.30	0.16	46 –115	51	313

Table 1 shows that the fixed threshold gives significantly better results with all the illumination techniques. The changes in the width and the twist of the fibers alter the amount of light reflected from the fiber to the camera, and thus cause changes in the gray level inside the fiber area in the images. Otsu's method often classifies these darker sections of the fibers as background. This is seen as commonly higher thresholds compared with the fixed values. However, the ranking between the performances of the illumination methods is the same with both of the thresholding methods.

The polarizer – analyzer configuration was superior to the other methods yielding clearly the highest detection ratios and the lowest breakage ratios. The results are excellent especially with the fixed thresholds. The ring light worked moderately but caused sometimes disturbing reflections from the substrate, and the contrast between the darkest sections of the fibers and the substrate was often too low. The operation of the dark light configuration was intolerable. Orientation of the fibers to the light sources affected the results but even the fibers perpendicular to the direction of light were poorly visible in the images. Clearly, the fibers were too transparent for this illumination type to work properly.

Scratches on the substrate might be detected as fibers as all of the illumination schemes are efficient in detecting unevenness. However, the microscope glass is a cheap and replaceable component, which does not damage easily in normal use. Thus, replacing the glass belongs to maintenance of the system, and analyzing the probabilities of this kind of false positives was excluded from the tests.

Since none of the illumination types studied was easily implementable to the microrobotic platform, the decision on the illumination method was made solely based on the performance. Thus, the polarizer – analyzer setup was implemented.

IV. IMPLEMENTING FINAL ILLUMINATION

Implementation of the polarizer – analyzer in the microrobotic test bench is challenging since it has to be integrated to the sample stage. However, the advantage is that the microgrippers cannot block the illumination unless they block also the view to the fiber samples. Integrating the light source and the polarizer into a sample stage, which is subject to rotation, is a challenging task for two reasons. First, the wiring of the backlight should not get twisted, and second, the angle of the polarizer should remain unchanged as the stage rotates. This requires using a stationary structure inside the rotating sample stage. Moreover, adding the light source, diffuser and polarizer on the rotary stage increases its height significantly. This makes moving samples from the rotary table to other locations on the xy stage, on which the force sensor and such components are attached, difficult due to the movement range of the grippers.

These problems were solved by using a three-level frame design and utilizing a hollow shaft of the rotary table. The bottom level serves as the attachment plate to the xy table and the anchor for the illumination system that should not rotate. The middle level is for attaching the rotary table, and the top level serves as the working plane. The light source, the diffuser and the polarizer are attached on a rod mounted on the bottom level and going through the middle level and

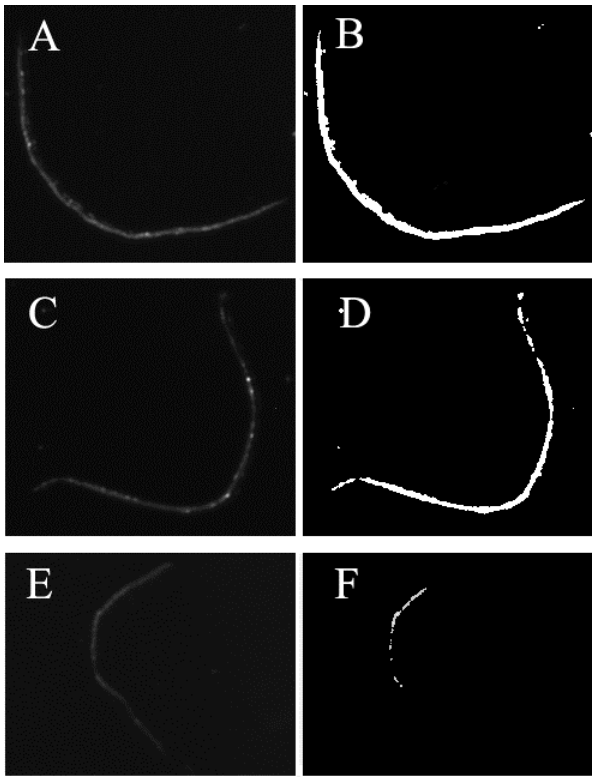

Figure 3. Different thresholding results. Intact fiber (B), broken fiber (D), and lost fiber (F). Original images (A, C, E), and thresholded binary images (B, D, F).

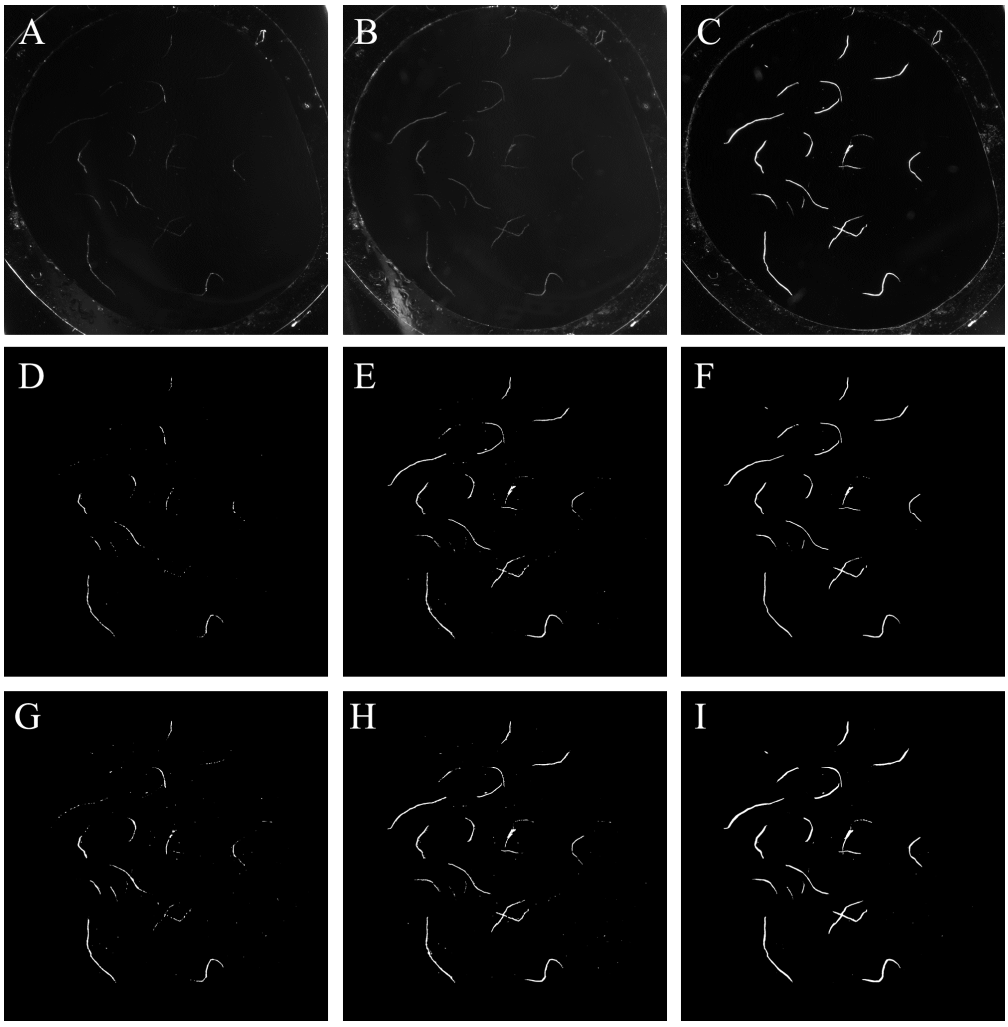

Figure 4. Images of wet fibers taken with different illumination (A – C) and binary images provided by Otsu's method (D – F) and the fixed threshold (G – I). Dark field (A, D, G), ring light (B, E, H) and polarizer – analyzer (C, F, I).

the hollow shaft of the rotary table. The wires of the light source are inside the rod. A hollow cylinder is used to transmit motion from the rotary table to the sample stage on the working plane. The cylinder is attached to the rotary table, and the uppermost section of the rod including the illumination system is placed inside. The top of the cylinder is removable and has a hole, on which a circular sample holder made of glass is mounted. A ring-shaped plastic sticker is utilized in creating the shallow pool needed for the fibers in suspension. The top level of the design has a hole for the cylinder and threads for attaching the force sensor. The parts were made of aluminum and the inner parts of the cylinder were made matte black to prevent reflections. The diffuser and the polarizer were attached on a black polyethylene tube surrounding the light source. Fig. 5 shows the design of the illumination system, and Fig. 6 presents the final implementation.

The performance of the final system was measured by using the same strategy as earlier. Totally 258 fibers were imaged and only a fixed threshold was utilized as it was found to be a better method. Table 2 presents the results. As it can be seen, the performance remained excellent.

TABLE II. PERFORMANCE OF THE FINAL DESIGN

r_{det}	r_{break}	n_{fibers}
0.99	0.10	258

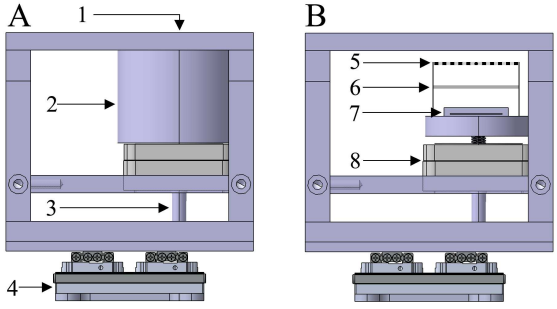

Figure 5. The final design of the polarizer system. The whole design (A), the cylinder removed (B). 1 – sample holder, 2 – cylinder, 3 – rod, 4 – xy table, 5 – polarizer, 6 – diffuser, 7 – light source and 8 – rotary table.

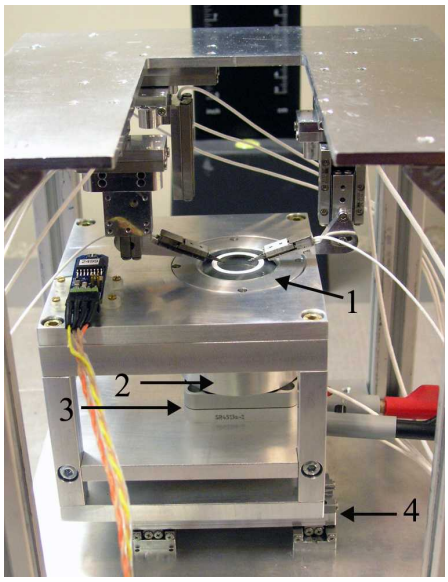

Figure 6. The final implementation. 1 – sample holder, 2 – cylinder, 3 – rotary table, 4 – xy table.

Also, real automatic fiber grasp and pick-up experiments have been completed with the developed illumination system and the results were good [20].

V. Conclusion

This paper presented the design and implementation of an illumination system usable in microrobotic studies of natural fibers. The system utilizes polarized light and in this study it was demonstrated with paper fibers. The proposed system provides excellent contrast between the fibers and the background. Therefore, 99% of paper fibers in the images taken with the developed illumination system in use can be detected by using simple thresholding. This is a superior result compared with the other illumination methods tested, dark field and ring light, which yielded 63% and 85% detected fibers, respectively. This high detection rate indicates that the system can be used for automated fiber detection, which is a key for automated fiber manipulation.

Implementing the illumination system on a stage that should provide both translation and rotation needed in manipulation tasks was demanding. However, the three-level design ensures that the movements are free from constraints.

As the illumination method requires transparency from the objects it is applied to, microgrippers and such actuators are not well visible while the system is in use. However, another illumination type, e.g. simple bright field illumination, can be used for locating the grippers. Also, the backlight of the developed illumination system can be used for detecting the silhouettes of the actuators by changing the analyzer angle to 0˚.

Acknowledgment

The authors would like to thank GETA (Graduate School of Electronics, Telecommunications and Automation) and the Academy of Finland (grant numbers 253364 and 256527) for their financial support.

References

[1] P. Saketi, A. Treimanis, P. Fardim, P. Ronkanen and P. Kallio, "Microrobotic platform for manipulation and flexibility measurement of individual paper fibers," in *Intelligent Robots and Systems (IROS), 2010 IEEE/RSJ International Conference On,* 2010, pp. 5762-5767.

[2] P. Saketi and P. Kallio, "Measuring bond strenghts of individual paper fibers using microrobotics," in *Progress in Paper Physics Seminar,* Graz, Austria, 2011, pp. 199-202.

[3] M. Probst, C. Hürzeler, R. Borer and B. J. Nelson, "A microassembly system for the flexible assembly of hybrid robotic mems devices," *International Journal of Optomechatronics,* vol. 3, pp. 69-90, 2009.

[4] U. Hirn and W. Bauer, "Review of image analysis based methods to evaluate fiber properties," *Lenzinger Berichte,* vol. 86, pp. 96-105, 2006.

[5] E. Tiikkaja, "Application of an optical fibre analyser and a tube flow fractionator to the estimation of quality potential of TMP: Experimental study," 2007.

[6] R. Eckhart, M. Donoser and W. Bauer, "Single fibre flexibility measurement in a flow cell based device," in *Proceedings of Advances in Paper Science and Technology (FRC),* 2009, .

[7] P. A. Reme, "Some effect of wood characteristics and the pulping process on mechanical pulp fibres," 2000.

[8] D. Coeurjolly and S. Svensson, "Estimation of curvature along curves with application to fibres in 3D images of paper," *Lecture Notes in Computer Science (Including Subseries Lecture Notes in Artificial Intelligence and Lecture Notes in Bioinformatics),* vol. 2749, pp. 247-254, 2003.

[9] M. Axelsson, "3D tracking of cellulose fibres in volume images," in *Proceedings - International Conference on Image Processing, ICIP,* 2006, pp. IV309-IV312.

[10] X. Deng, X. Ye, J. Fang, C. Lin and L. Wang, "Surface defects inspection system based on machine vision," in *Proceedings - International Conference on Electrical and Control Engineering, ICECE 2010,* 2010, pp. 2205-2208.

[11] N. Wei, J. You, K. Friehs, E. Flaschel and T. W. Nattkemper, "In situ dark field microscopy for on-line monitoring of yeast cultures," *Biotechnol. Lett.,* vol. 29, pp. 373-378, 2007.

[12] E. Langlais, S. Adudodla and P. Mehta, "Using machine vision based system for benchmarking various printing plate surfaces," in *International Conference on Digital Printing Technologies,* 2003, pp. 595-597.

[13] V. Heiskanen, K. Marjanen and P. Kallio, "Machine Vision Based Measurement of Dynamic Contact Angles in Microchannel Flows," *Journal of Bionic Engineering,* vol. 5, pp. 282-290, 2008.

[14] H. Axer, M. Axerl, T. Krings and D. G. v. Keyserlingk, "Quantitative estimation of 3-D fiber course in gross histological sections of the human brain using polarized light," *J. Neurosci. Methods,* vol. 105, pp. 121-131, 2001.

[15] J. Rieppo, J. Hallikainen, J. S. Jurvelin, I. Kiviranta, H. J. Helminen and M. M. Hyttinen, "Practical considerations in the use of polarized light microscopy in the analysis of the collagen network in articular cartilage," *Microsc. Res. Tech.,* vol. 71, pp. 279-287, 2008.

[16] C. Ye, M. O. Sundstrom and K. Remes, "Microscopic transmission ellipsometry: measurement of the fibril angle and the relative phase retardation of single, intact wood pulp fibers," *Appl. Opt.,* vol. 33, pp. 6626-6637, 1994.

[17] L. Kappel, U. Hirn, E. Gilli, W. Bauer and R. Schennach, "Revisiting polarized light microscopy for fiber-fiber bond area measurement - Part I: Theoretical fundamentals," *Nordic Pulp and Paper Research Journal,* vol. 25, pp. 65-70, 2010.

[18] N. Otsu, "A Threshold Selection Method from Gray-Level Histograms," *Systems, Man and Cybernetics, IEEE Transactions On,* vol. 9, pp. 62-66, 1979.

[19] M. Sezgin and B. Sankur, "Survey over image thresholding techniques and quantitative performance evaluation," *Journal of Electronic Imaging,* vol. 13, pp. 146-168, January 1, 2004.

[20] M. von Essen, J. Hirvonen, S. Kuikka and P. Kallio, "Towards fully automated pick and place operations of individual natural fibers," in *3M-Nano,* Suzhou, China, 2013.